Dalton Transactions

ROYAL SOCIETY OF CHEMISTRY

PAPER

View Article Online
View Journal

Check for updates

Cite this: DOI: 10.1039/d0dt01338b

N_3-Ligated nickel(II) diketonate complexes: synthesis, characterization and evaluation of O_2 reactivity†

Josiah G. D. Elsberg,[a] Austin Peterson,[a] Amy L. Fuller[b] and Lisa M. Berreau *[a]

Interest in O_2-dependent aliphatic carbon–carbon (C–C) bond cleavage reactions of first row divalent metal diketonate complexes stems from the desire to further understand the reaction pathways of enzymes such as DKE1 and to extract information to develop applications in organic synthesis. A recent report of O_2-dependent aliphatic C–C bond cleavage at ambient temperature in Ni(II) diketonate complexes supported by a tridentate nitrogen donor ligand [(MBBP)Ni(PhC(O)CHC(O)Ph)]Cl (**7-Cl**; MBBP = 2,6-bis(1-methylbenzimidazol-2-yl)pyridine) in the presence of NEt_3 spurred our interest in further examining the chemistry of such complexes. A series of new TERPY-ligated Ni(II) diketonate complexes of the general formula [(TERPY)Ni(R_2-1,3-diketonate)]ClO_4 (**1**: R = CH_3; **2**: R = $C(CH_3)_3$; **3**: R = Ph) was prepared *under air* and characterized using single crystal X-ray crystallography, elemental analysis, ^{1}H NMR, ESI-MS, FTIR, and UV-vis. Analysis of the reaction mixtures in which these complexes were generated using ^{1}H NMR and ESI-MS revealed the presence of both the desired diketonate complex and the bis-TERPY derivative $[(TERPY)_2Ni](ClO_4)_2$ (**4**). Through selective crystallization **1–3** were isolated in analytically pure form. Analysis of reaction mixtures leading to the formation of the MBBP analogs [(MBBP)Ni(R_2-1,3-diketonate)]X (X = ClO_4: **5**: R = CH_3; **6**: R = $C(CH_3)_3$; **7-ClO$_4$**: R = Ph; X = Cl: **7-Cl**: R = Ph) using ^{1}H NMR and ESI-MS revealed the presence of $[(MBBP)_2Ni](ClO_4)_2$ (**8**). Analysis of aerobic acetonitrile solutions of analytically pure **1–3**, **5** and **6** containing NEt_3 and in some cases H_2O using ^{1}H NMR and UV-vis revealed evidence for the formation of additional bis-ligand complexes (**4** and **8**) but suggested no oxidative diketonate cleavage reactivity. Analysis of the organic products generated from **3**, **7-ClO$_4$** and **7-Cl** revealed unaltered dibenzoylmethane. Our results therefore indicate that N_3-ligated Ni(II) complexes of unsubstituted diketonate ligands do not exhibit O_2-dependent aliphatic C–C bond clevage at room temperature, including in the presence of NEt_3 and/or H_2O.

Received 11th April 2020,
Accepted 18th May 2020

DOI: 10.1039/d0dt01338b

rsc.li/dalton

Published on 19 May 2020. Downloaded by Utah State University on 5/28/2020 4:39:59 PM.

Introduction

Oxidative aliphatic carbon–carbon (C–C) bond cleavage reactions mediated by first row metals using O_2 as the terminal oxidant are of significant current interest, particularly for applications in organic synthesis.[1–7] To date, examination of the mechanistic pathways of these reactions has received minimal attention. This is due in part to the limited number of systems wherein a well-characterized metal/substrate type structure can be evaluated in terms of its O_2 reactivity. A few laboratories have developed model systems for enzymes that mediate O_2-dependent aliphatic C–C bond cleavage. DKE1 is an enzyme found in *Acinetobacter johnsonii* which catalyzes the oxidative cleavage of diketonate substrates, including acetylacetone, using O_2 as the terminal oxidant.[8] The active site of DKE1 contains a non-heme Fe(II) center ligated in a facial array by three histidine donors (Scheme 1(a)).[9–11] Siewert *et al.* used a trispyrazolylborato (Tp) ligand to mimic the 3His facial triad in a Fe(II) diethylphenylmalonate complex (Scheme 1(b)).[12] This complex undergoes O_2-dependent aliphatic C–C cleavage within the diketonate unit to give ethyl carbonate (which decomposes to give CO_2 and ethoxide anion) and ethyl benzoylformate as products of a dioxygenase-type reaction. Park *et al.* reported a similar set of complexes using two different ^{R_2}Tp ligands (R = –Me and –Ph; Scheme 1(c)) and a variety of diketonate ligands.[13] Their studies showed that O_2-dependent cleavage only occurred for ^{Ph_2}Tp complexes containing a

[a]Department of Chemistry & Biochemistry, Utah State University, 0300 Old Main Hill, Logan, UT 84322-0300, USA. E-mail: lisa.berreau@usu.edu
[b]Department of Chemistry, University of Hawaii Manoa, 2545 McCarthy Mall, Honolulu, HI 96822-2275, USA

†Electronic supplementary information (ESI) available: Paramagnetic ^{1}H NMR, ESI-MS, and FT-IR spectra; crystallographic data; organic recovery data. CCDC 1991784, 1991786, 1991787 and 1992287. For ESI and crystallographic data in CIF or other electronic format see DOI: 10.1039/d0dt01338b

Published on 19 May 2020. Downloaded by Utah State University on 5/28/2020 4:39:59 PM.

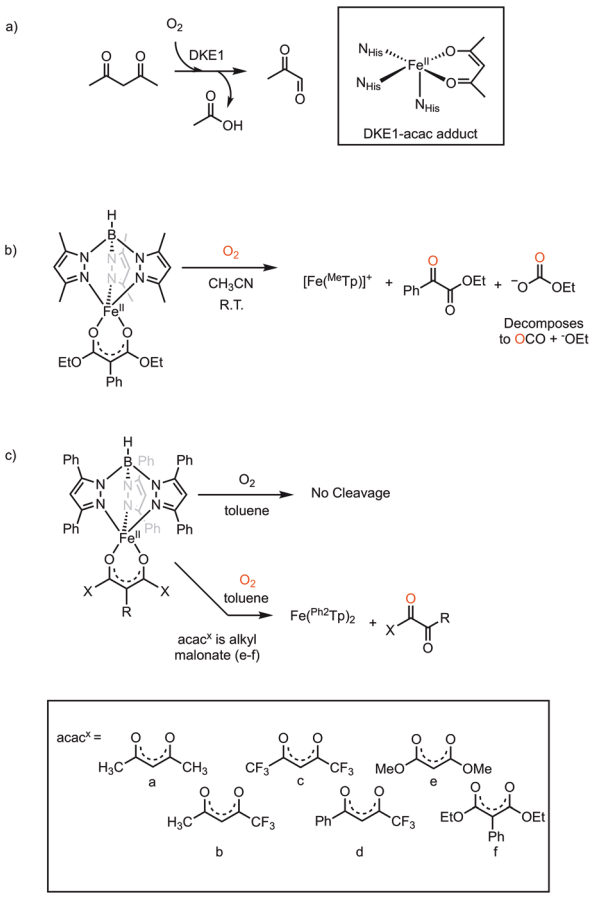

Scheme 1 a) Reaction catalyzed and active site iron center of DKE1. (b) Diethylphenylmalonate-containing model complex for the active site of DKE1. (c) Complexes with diketonates e–f undergo oxidative C–C bond cleavage whereas those with diketonates a–d do not exhibit this reactivity.

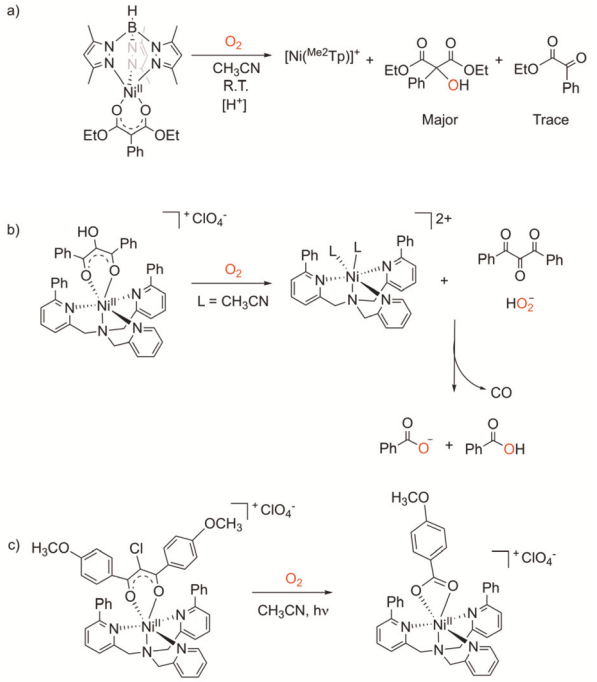

Scheme 2 a) Reaction of a ^{Me_2}TpNi(II) diethylphenylmalonate complex with O_2. (b) Reactivity of Ni(II) hydroxydiketonate complex that mimics the reactivity of Ni(II)-containing acireductone dioxygenase (ARD). (c) UV-light induced aliphatic C–C bond cleavage of methoxy-substituted chlorodiketonate complex in the presence of O_2.

diethyl malonate or diethylphenylmalonate diketonate ligand. Complexes that didn't undergo oxidative diketonate cleavage exhibited either no reaction or formed a green peroxo-bridged intermediate that decayed without any oxidative C–C bond cleavage. Recently, Banerjee and Paine reported that an Fe(II) dibenzoylmethane complex supported by the monoanionic tris (2-pyridylthio)methanido ligand undergoes reaction with O_2 at ambient temperature to give a small amount of benzoic acid (11–13%).[14] The major product of this reaction is the Fe(III) diketonate complex.

To examine how a change in the metal center affects O_2 activation, Hoof *et al.* studied the O_2 reactivity of a ^{Me_2}Tp-ligated Ni (II) diethylphenylmalonate complex.[15] Their studies revealed O_2-dependent reactivity leading to hydroxylation and aliphatic C–C bond cleavage products (Scheme 2(a)). This reaction required an open coordination position at the Ni(II) center as using the more sterically hindered ^{Ph_2}Tp supporting ligand system did not produce the same type of reactivity. A hydroxylated diphenyl diketonate ligand in a model system for Ni(II)-containing acireductone dioxygenase (Scheme 2(b)) undergoes two-electron oxidation upon reaction with O_2 to give a triketone and hydroperoxide anion as intermediates.[16,17] Subsequent reaction between these intermediates in the presence of the remaining Ni(II) complex gives benzoate/benzoic acid and CO as products of the aliphatic C–C bond cleavage reaction. An Fe (II) analog produces similar products as well as an α-keto acid product, which results from iron-promoted hydration of the triketone intermediate followed by C–C cleavage.[18] Recently, Raje, *et al.* reported similar results using a Ni(II) complex supported by a tetradentate pyridinophane (L_4) ligand.[19] This complex was treated with the hydroxylated dibenzoylmethane (PhC(O)C (OH)C(O)Ph) in the presence of base in CH_3CN. Exposure of this solution to O_2 followed by ESI-MS analysis revealed the presence of the $[L_4Ni(OC(O)Ph)]^+$ cation. Organic recovery experiments also revealed the formation of benzoic acid. These results mirror those previously reported by Szajna *et al.*[16]

Notably, a structurally similar Ni(II) dibenzoylmethane complex that does not contain the hydroxyl substituent on the central carbon of the diketonate ligand is air stable.[20] However, a Ni(II) chlorodiketonate complex having methoxy-substituted phenyl appendages (Scheme 2(c)) undergoes O_2-dependent aliphatic C–C bond cleavage reactivity within the diketonate moiety to give a carboxylate product upon illumination with UV light.[21] This reactivity is similar to thermal oxidative C–C bond cleavage identified for structurally-similar copper chlorodiketonate complexes.[22,23]

Based on the literature precedent described above, which shows that only electron rich diketonates, or those containing

This journal is © The Royal Society of Chemistry 2020

Published on 19 May 2020. Downloaded by Utah State University on 5/28/2020 4:39:59 PM.

a central carbon substituent that can undergo reaction or act as a leaving group, exhibit significant O_2 reactivity, a recent publication drew our attention.[24] Ramasubramanian, *et al.* reported that Ni(II) diketonate complexes (Scheme 3(a)) supported by the tridentate 2,6-bis(1-methylbenzoimidazol-2-yl) pyridine (MBBP) ligand undergo O_2-dependent oxidative cleavage in the presence of one equivalent of triethylamine (NEt_3) and in the absence or presence of water (10% in CH_3CN) (Scheme 3(b)) to give carboxylic acid products (52%, R = Ph) along with CO_2. These reactions are reported to occur under mild conditions, as a 6.00×10^{-4} M solution of each complex undergoes complete reaction in <1 h at 25 °C as determined by UV-vis. $^{18}O_2$ studies showed 43% isotope incorporation in the benzoic acid product. A reaction pathway was proposed for the R = Ph derivative (Scheme 3(b)) wherein the diketonate acts as a two-electron reductant to O_2, leading to the formation of an organoperoxo species that is stabilized *via* interaction with Ni(II). Intramolecular attack of the terminal peroxo oxygen at a diketonate carbonyl moiety followed by aliphatic C–C bond cleavage gives the benzoic acid product and phenylgloyoxal. Another report in the literature suggested that O_2-dependent oxidative cleavage of an acetylacetonate ligand can occur in $Ni(acac)_2(H_2O)_2$ the presence of base (ethylenediamine) (Scheme 3(c)).[25] However, this reaction was reported to proceed very slowly at room temperature (18 d under air).

The reactions outlined in Scheme 3 are interesting in that aliphatic C–C cleavage is reported to occur within an unsubstituted diketonate under mild conditions, which is rare to date in synthetic systems. Based on these results we became interested in further examining such systems. Herein we report synthetic, characterization and reactivity studies of a series of new TERPY-ligated Ni(II) diketonate complexes, [(TERPY)Ni(diketonate)]ClO_4 (**1–3**). While such complexes could be isolated by selective crystallization, the reaction mixtures leading to their formation always also contained $[(TERPY)_2Ni](ClO_4)_2$ (**4**). Unlike the MBBP Ni(II) diketonate complexes reported by Ramasubramanian, *et al.*,[24] **1–3** are stable with respect to O_2 over 24 h, showing no aliphatic C–C bond cleavage reactivity upon exposure to air, even in the presence of base and water. Based on these results, we re-examined the chemistry of the MBBP-ligated diketonate complexes. Using ^{1}H NMR under paramagnetic conditions we found that the formation of a bis-MBBP Ni(II) complex is prevalent under the reaction conditions.[24,26] Ramasubramanian *et al.* briefly mention this complex, but did not report the chemistry associated with such species. Using an organic recovery experiment, we found no evidence for oxidative aliphatic C–C bond cleavage upon exposure of [(MBBP)Ni(PhC(O)CHC(O)Ph)]X (**7-X**; X = Cl or ClO_4) to O_2 in the presence of NEt_3 or NEt_3/H_2O after 24 h.

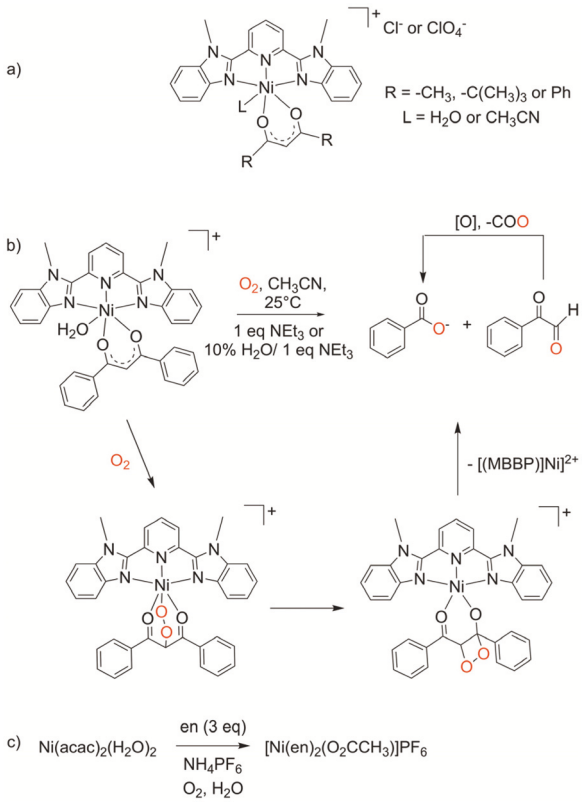

Scheme 3 a) MBBP-ligated Ni(II) diketonate complexes reported by Ramasubramanian, *et al.*[24] (b) Proposed pathway of O_2 reaction of MBBP-ligated Ni(II) phenyl diketonate complex. (c) Oxidative cleavage of an aceytylacetonate ligand.[25]

Experimental

General methods

The following chemicals were purchased and used as received: 1,3-diphenylpropane-1,3-dione (98%, Sigma-Aldrich), 2,4-pentanedione (99%, Acros Organics), 2,2,6,6-tetramethyl-3,5-heptanedione (97%, Combi-Blocks) and 2,2′;6′,2″-terpyridine (98%, Sigma-Aldrich). Solvents used in air were used without further purification unless otherwise stated. Solvents used in the glovebox were dried following a previously published procedure prior to use.[27] The CD_3CN used in ^{1}H NMR experiments was dried using molecular sieves. 2,6-Bis(2′-benzimidazolyl)pyridine (BBP) was prepared following the literature procedure.[28] Manipulations performed under an inert N_2 atmosphere were conducted in a MBraun Unilab glovebox.

Physical methods

^{1}H NMR spectra were collected on a Brüker Advance III HD Ascend-500 spectrometer. Chemical shifts (ppm) are reported relative to the residual solvent peak in CD_2HCN (1.94 ppm, quintet) or $CHCl_3$ (7.26 ppm, singlet). ^{1}H NMR spectra for high-spin paramagnetic Ni(II) complexes were collected using previously published parameters: 32k data points, 300 scans, a 90° pulse (9.75 μs) at 298 K, and a 250 ms relaxation delay.[26] During processing, an exponential weighting function (lb = 7 Hz) and a manual baseline correction were performed using MNova (Version 12.0.4). FTIR spectra were collected as KBr pellets using a Shimadzu FTIR-8400 spectrometer. UV-vis data

Published on 19 May 2020. Downloaded by Utah State University on 5/28/2020 4:39:59 PM.

was collected using a Hewlett-Packard 8453A diode array spectrometer at ambient temperature. ESI mass spectral data was collected using a Shimadzu LCMS-2020. Elemental analyses were performed by Robertson Microlit Laboratories (Ledgewood, NJ) or Atlantic Microlab (Norcross, GA).

Caution! Perchlorate compounds containing organic ligands are potentially explosive. These materials should be handled with care and in small quantities.[29]

Synthesis and characterization. Unless stated otherwise all synthetic reactions were performed in air.

[(TERPY)Ni($CH_3C(O)CHC(O)CH_3$)(CH_3CN)]ClO_4 (1). Ni$(ClO_4)_2{\cdot}6H_2O$ (49.4 mg 0.135 mmol) was dissolved in CH_3CN (2 mL) under air. An excess of 2,4-pentanedione (~1 mL) and one equivalent of triethylamine (19 μL, 0.135 mmol) were subsequently added. The mixture was then stirred for approximately 30 min during which time it became blue. This solution was added to a vial containing TERPY (31.6 mg, 0.135 mmol) dissolved in CH_3CN (2 mL). The resulting solution became faint yellow. After stirring at ambient temperature for 2 h, Et_2O (8 mL) was added and the solution was placed in the freezer (−15 °C) for 12 h. This produced grayish-green X-ray quality crystals. We note that the ratio of Et_2O to CH_3CN (~1.4 : 1) is important to selectively crystallize **1**. The solution was decanted from the crystals, which were then washed with Et_2O and dried under vacuum (49 mg, 74% yield). ESI-MS: *m*/*z* calc. for $C_{20}H_{18}N_3NiO_2{\cdot}CH_3CN$, 431.1 $[M - ClO_4]^+$; found 431.0; calc. 390.1 $[M - CH_3CN - ClO_4]^+$; found 390.0. Anal. calc. for $C_{20}H_{18}ClN_3NiO_6{\cdot}CH_3CN$: C, 49.71; H, 3.98; N, 10.54. Found: C, 49.34; H, 3.92; N, 10.35. UV-Vis λ_{max}, nm (ε, M^{-1} cm^{-1}): 233 (23 532), 272 (17 307), 279 (19 884), 305 (18 457), 319 (17 046), 329 (13 074). FT-IR (KBr, cm^{-1}): 3420 (ν_{O-H}), 3100 (ν_{C-H}), 2320 ($\nu_{C\equiv N}$), 2020 (ν_{C-H}), 1600 ($\nu_{C=C}$), 1520 ($\nu_{C=N}$), 1450 ($\nu_{C=O}$), 1400 ($\nu_{C=O}$), 1090 (ν_{ClO_4}), 780 (ν_{C-H}), 620 (ν_{ClO_4}).

[(TERPY)Ni((CH_3)$_3$CC(O)CHC(O)C(CH_3)$_3$)(H_2O)]ClO_4 (2). Ni$(ClO_4)_2{\cdot}6H_2O$ (49.4 mg 0.135 mmol) was dissolved in CH_3CN (2 mL) under air. An excess of 2,2,6,6-tetramethyl-3,5-heptanedione (141 μL, 0.675 mmol) was added, along with triethylamine (19 μL, 0.135 mmol). The resulting solution was stirred for 30 min, during which time it became blue. This solution was then added to a vial containing TERPY (31.6 mg, 0.135 mmol) dissolved in CH_3CN (2 mL). The resulting yellow-green mixture was stirred for 2 h. Et_2O (8 mL) was added and the solution was placed in the freezer (−15 °C) overnight which resulted in the deposition of a fine tan precipitate (**4** by ^{1}H NMR; *vida infra*). The yellow-green solution was brought to dryness under reduced pressure. Crystalline material was obtained by dissolving the precipitate in CH_2Cl_2, adding a few drops of CH_3CN, followed by slow diffusion of Et_2O (41 mg, 53% yield). ESI-MS: *m*/*z* calc. for $C_{26}H_{30}N_3NiO_2{\cdot}CH_3CN$, 515.2 $[M - ClO_4]^+$; found 515.2; calc. 474.2 $[M - CH_3CN - ClO_4]^+$; found 474.1. Anal. calc. for $C_{26}H_{30}ClN_3NiO_6{\cdot}H_2O{\cdot}0.9\ CH_2Cl_2$: C, 48.28; H, 5.09; N, 6.28. Found: C, 48.48; H, 4.89; N, 6.54. UV-Vis λ_{max}, nm (ε, M^{-1} cm^{-1}): 233 (27 182), 270 (18 653), 278 (22 176), 306 (21 052), 316 (23 235), 328 (14 948). FT-IR (KBr, cm^{-1}): 3530 (ν_{O-H}), 3430 (ν_{O-H}), 2960 (ν_{C-H}), 2020 (ν_{C-H}), 1590 ($\nu_{C=C}$), 1410 ($\nu_{C=O}$), 1110 (ν_{ClO_4}), 780 (ν_{C-H}), 630 (ν_{ClO_4}).

[(TERPY)Ni(Ph(O)CHC(O)Ph)(H_2O)]ClO_4 (3). Ni$(ClO_4)_2{\cdot}6H_2O$ (49.4 mg 0.135 mmol) was dissolved in CH_3CN (2 mL) under air. Dibenzoylmethane (30.1 mg, 0.135 mmol) was added to the solution along with triethylamine (19 μL, 0.135 mmol). This mixture was stirred for 30 minutes and then added to a vial containing TERPY (31.6, 0.135 mmol) dissolved in CH_3CN (2 mL). The resulting solution was stirred for 2 h during which time it became green. Excess Et_2O (8 mL) was added and the solution was placed in the freezer (−15 °C) overnight. The yellow-green solution was decanted away from a tan solid (**4** by ^{1}H NMR; *vida infra*) and was brought to dryness under reduced pressure. The resulting thick green oil was dissolved in CH_2Cl_2 (4 mL) and the solution was passed through a Celite plug. Slow diffusion of Et_2O into the CH_2Cl_2 filtrate produced X-ray diffraction quality crystals (35 mg, 42% yield). ESI-MS: *m*/*z* calc. for $C_{30}H_{22}N_3NiO_2{\cdot}CH_3CN$, 555.1 $[M - ClO_4]^+$; found 555.2; calc. 514.1 $[M - CH_3CN - ClO_4]^+$; found 514.1. Anal. calc. for $C_{30}H_{22}ClN_3NiO_6{\cdot}H_2O$: C, 56.95; H, 3.82; N, 6.64. Found: C, 57.08; H, 3.75; N, 6.70. UV-Vis λ_{max}, nm (ε, M^{-1} cm^{-1}): 236 (20 752), 253 (17 386), 270 (17 553), 278 (18 609), 317 (12 050), 329 (13 187), 364 (10 790) (d–d transitions). FT-IR (KBr, cm^{-1}): 3440 (ν_{O-H}), 3160 (ν_{C-H}), 2010 (ν_{C-H}), 1600 ($\nu_{C=C}$), 1510 ($\nu_{C=N}$), 1450 ($\nu_{C=O}$), 1410 ($\nu_{C=O}$), 1090 (ν_{ClO_4}), 780 (ν_{C-H}), 630 (ν_{ClO_4}).

[(TERPY)$_2$Ni](ClO_4)$_2$ (4). This compound has been previously reported but a new synthesis is provided here.[30,31] A mixture of Ni$(ClO_4)_2{\cdot}6H_2O$ (24.7 mg 0.0675 mmol) and TERPY (31.5 mg, 0.135 mmol) in CH_3CN (5 mL) was stirred for 12 h under air at ambient temperature. Slow diffusion of Et_2O into the CH_3CN solution produced orange-brown plates. (31 mg, 63% yield). ESI-MS: *m*/*z* calc. for $[C_{30}H_{22}N_6Ni{\cdot}ClO_4]^+$, 623.1; found, 623.1; calc. 262.1 $[M\text{-}(2{\cdot}ClO_4)]^{2+}$; found 262.1. Anal. calc. for $C_{30}H_{22}Cl_2N_6NiO_8{\cdot}H_2O$: C, 48.55; H, 3.26; N, 11.32. Found: C, 48.38; H, 2.95; N, 11.30. UV-Vis λ_{max}, nm (ε, M^{-1} cm^{-1}): 235 (31 872), 269 (29 970), 310 (18 235), 320 (27 374), 334 (25 642). FT-IR (KBr, cm^{-1}): 3610 (ν_{O-H}), 3410 (ν_{O-H}), 3120 (ν_{C-H}), 2360 (ν_{C-N}), 2010 (ν_{C-H}), 1610 ($\nu_{C=C}$), 1450 ($\nu_{C=O}$), 1090 (ν_{ClO_4}), 770 (ν_{C-H}), 620 (ν_{ClO_4}).

Analysis of crystallization filtrates by ^{1}H NMR. Crystallization of **1–3** produced materials with purity as determined by elemental analysis. Evaluation of the remaining filtrates by ^{1}H NMR revealed the presence of **4** in each reaction mixture.

Addition of TERPY (1 eq.) to 1 in CD_3CN. Complex **1** (4.30×10^{-3} mmol) was dissolved in CD_3CN (600 μL), and a ^{1}H NMR spectrum was collected under paramagnetic conditions. TERPY (4.30×10^{-3} mmol) was added, the solution was briefly mixed and another ^{1}H NMR spectrum was collected. Additional spectra were collected after 3 h and 24 h. The NMR spectra indicated significant formation of **4**.

Probing for aliphatic C–C bond cleavage reactivity involving 3. Complex **3** (10 mg, 0.02 mmol) was dissolved in CH_3CN (2.7 ml) in a glass scintillation vial with a stir bar. Following the addition of H_2O (300 μL) and NEt_3 (279 μL, 2.00 mmol) and purging with O_2 for 1 min, the mixture was stirred for 24 h. The solvent was then removed under reduced pressure.

 This journal is © The Royal Society of Chemistry 2020

Published on 19 May 2020. Downloaded by Utah State University on 5/28/2020 4:39:59 PM.

CH_2Cl_2 (8 ml) and HCl (8 ml, 1 M) were added, followed by stirring for 1 h and subsequently the organic layer was separated. The organic layer was dried over Na_2SO_4 and brought to dryness under vacuum to give a white solid (3.2 mg, 71% based on dibenzoylmethane). The ^{1}H NMR ($CDCl_3$) spectrum of the solid showed only dibenzoylmethane and no aliphatic C–C bond cleavage products.

In a separate experiment, a similar reaction was performed with the only difference being **3** (10 mg, 0.02 mmol) was dissolved in dry CH_3CN (3 mL) and one equivalent of NEt_3 (~3 μL, 0.02 mmol) was added. An aliquot was removed before O_2 purge and after stirring for an additional 24 h. ESI-MS of both aliquots only contained patterns for **3** and **4**. After workup, a white solid was collected (4.1 mg, 91%). The ^{1}H NMR of this solid indicated recovery of dibenzoylmethane.

2,6-Bis(1-methylbenzimidazol-2-yl)pyridine (MBBP). This procedure includes slight modifications from the previously published synthesis.[28] 2,6-Bis(2′-benzimidazolyl)pyridine (1.00 g, 3.21 mmol) was added to a round bottom flask containing acetone (30 mL) and powdered potassium hydroxide (0.90 g, 16 mmol). This mixture was stirred at room temperature for 30 min during which time it became brown-red. Methyl iodide (0.60 ml, 9.6 mmol) was added and the reaction stirred overnight. Following the addition of water, a light tan precipitate was produced. This solid was removed *via* filtration, dissolved in dichloromethane, and the solution was dried over sodium sulfate. Following filtration to remove the drying agent, the filtrate was collected and brought to dryness under reduced pressure to give a tan solid (0.50 g, 46% yield). ^{1}H NMR ($CDCl_3$) δ (ppm): 8.40 (d, 2H, 8.5 Hz), 8.04 (t, 1H, 7.9 Hz), 7.87 (d, 2H, 7.9), 7.46 (d, 2H 7.37 Hz), 7.36 (m, 4H), 4.24 (s, 6H). These ^{1}H NMR features match those previously reported.[28]

Synthesis of [(MBBP)Ni(CH_3C(O)CHC(O)CH_3)]ClO_4 (5) and [(MBBP)Ni((CH_3)$_3$CC(O)CHC(O)C(CH_3)$_3$)]ClO_4 (6). These complexes were prepared under air. $Ni(ClO_4)_2{\cdot}6H_2O$ (24.7 mg, 0.0675 mmol) was dissolved in CH_3CN (2 mL). The diketone, 2,4 pentanedione (7.0 μL, 0.0675 mmol) or 2,2,6,6-tetramethyl-3,5-heptanedione (13.8 μL, 0.0675 mmol), was added along with triethylamine (9.4 μL, 0.0675 mmol). The resulting blue solution was stirred for 30 min at ambient temperature. MBBP (22.9 mg, 0.0675 mmol) dissolved in CH_3CN (2 mL) was added, which resulted in the precipitation of a green solid. This solid was carefully collected and dried by gravity filtration using a Buchner funnel and filter paper (**5**: 19 mg, 46%; **6**: 18 mg, 40%). ^{1}H NMR analysis of each solid indicated the presence of a single compound. **5**: ESI-MS: *m*/*z* calc. for $C_{26}H_{24}N_5NiO_2{\cdot}CH_3CN$, 537.2 $[M - ClO_4]^+$; found 537.1; 496.1 $[M - CH_3CN - ClO_4]^+$; found 496.3. Anal. calc. for $C_{26}H_{24}ClN_5NiO_6$: C, 52.34; H, 4.05; N, 11.74. Found: C, 52.28; H, 4.11; N, 11.66. UV-Vis λ_{max}, nm (ε, M^{-1} cm^{-1}): 249 (13 720), 304 (40 254), 350 (22 999), 366 (16 041). FT-IR (KBr, cm^{-1}): 3440 (ν_{O-H}), 3120 (ν_{C-H}), 2360 (ν_{C-N}), 2030 (ν_{C-H}), 1930 (ν_{C-H}), 1600 ($\nu_{C=C}$), 1400 ($\nu_{C=O}$), 1110 (ν_{ClO_4}), 750 (ν_{C-H}), 620 (ν_{ClO_4}). **6**: ESI-MS: *m*/*z* calc. for $C_{32}H_{36}N_5NiO_2{\cdot}CH_3CN$, 621.3 $[M - ClO_4]^+$; found 621.2; calc. 580.2 $[M - CH_3CN - ClO_4]^+$; found 580.2. Anal. calc. for $C_{32}H_{36}ClN_5NiO_6{\cdot}0.4\ H_2O$: C, 55.61; H, 5.34; N, 10.12. Found: C, 55.86; H, 5.39; N, 10.18. UV-Vis λ_{max}, nm (ε, M^{-1} cm^{-1}): 249 (11 864), 305 (29 644), 348 (17 675), 366 (10 896). FT-IR (KBr, cm^{-1}): 3410 (ν_{O-H}), 3150 (ν_{C-H}), 2980 (ν_{C-H}), 2020 (ν_{C-H}), 1590 ($\nu_{C=C}$), 1410 ($\nu_{C=O}$), 1120 (ν_{ClO_4}), 750 (ν_{C-H}), 630 (ν_{ClO_4}).

Analysis of filtrates. Analysis of the filtrates remaining following removal of the green solids of **5** and **6** using ^{1}H NMR and ESI-MS revealed the presence of the diketonate complexes (**5** and **6**) as well as $[(MBBP)_2Ni](ClO_4)_2$ (**8**), which was independently synthesized and characterized (*vida infra*).

Synthesis of 6 following previously published procedures. Under N_2, $Ni(ClO_4)_2{\cdot}6H_2O$ (24.7 mg, 0.0675 mmol) was dissolved in CH_3CN (2 mL). 2,2,6,6-tetramethyl-3,5-heptanedione (13.8 μL, 0.0675 mmol) and triethylamine (9.4 μL, 0.0675 mmol) were then added to the vial and stirred for 30 minutes. MBBP (22.9 mg, 0.0675 mmol) dissolved in CH_3CN (2 mL) was added, which resulted in the precipitation of a green solid. This solution was stirred for 2 h, then Et_2O (8 mL) was added to the mixture. This mixture was then placed in the freezer overnight (−12 °C). The green precipitate collected on the bottom, so the solution was decanted off and the precipitate washed with more Et_2O and dried. The ^{1}H NMR under paramagnetic conditions and the ESI-MS of the solid indicated that **6** is present along with **8**.

Attempted synthesis of [(MBBP)Ni(PhC(O)CHC(O)Ph)]ClO_4 (7-ClO_4). The previously reported synthesis was followed in an attempt to make this complex.[24] $Ni(ClO_4)_2{\cdot}6H_2O$ (24.7 mg, 0.0675 mmol) was dissolved in CH_3CN (~2 mL). This solution was combined with dibenzoylmethane (15.2 mg, 0.0675 mmol) and triethylamine (9.4 μL, 0.0675 mmol). The resulting mixture was stirred for 30 min at which point it was transferred to vial containing MBBP (22.9 mg, 0.0675 mmol). This resulted in the formation of a clear green solution. After stirring for 2 h, Et_2O (8 mL) was added, which resulted in the deposition of a green-yellow precipitate. The solid was collected and dried under vacuum. ESI-MS (CH_3CN) and ^{1}H NMR (CD_3CN) showed that both [(MBBP)Ni(PhC(O)CHC(O)Ph)]ClO_4 (7-ClO_4) and **8** were present. We were unable to selectively precipitate 7-ClO_4 as had been possible with **5** and **6**.

Attempted synthesis of [(MBBP)Ni(PhC(O)CHC(O)Ph)]Cl (7-Cl). To a solution of $NiCl_2$ (16.0 mg, 0.0675 mmol) in CH_3CN (2 mL) was added dibenzoylmethane (15.2 mg, 0.0675 mmol) and triethylamine (9.4 μL, 0.0675 mmol). The mixture was stirred for about 30 min at which point it was added to a vial containing MBBP (22.9 mg, 0.0675 mmol). A green precipitate formed which was separated by filtration (11.3 mg). Analysis of this solid by ^{1}H NMR (d_6-DMSO) showed the presence of a mixture of 7-**Cl** and **8**. Analysis of the filtrate by ^{1}H NMR (d_6-DMSO) also showed the presence of both complexes. We were unable to selectively crystallize 7-**Cl** as was possible with **5** and **6**.

Synthesis of $[(MBBP)_2Ni](ClO_4)_2$ (8). $Ni(ClO_4)_2{\cdot}6H_2O$ (12.4 mg, 0.0338 mmol) was combined with MBBP (22.9, 0.0675) in CH_3CN (3 mL). This solution was stirred for 12 h at room temperature. Slow diffusion of Et_2O into the CH_3CN

Published on 19 May 2020. Downloaded by Utah State University on 5/28/2020 4:39:59 PM.

solution produced small brown crystals suitable for single crystal X-ray crystallographic characterization. (26 mg, 83% yield). ESI-MS: *m*/*z* calc. for $C_{42}H_{34}N_{10}Ni{\cdot}ClO_4$, 835.1 $[M - ClO_4]^+$, found 835.2, calc. 368.1 $[M - (2ClO_4)]^{2+}$; found 368.5. Anal. calc. for $C_{42}H_{34}Cl_2N_{10}NiO_8{\cdot}0.4\ H_2O$: C, 53.46; H, 3.71; N, 14.84. Found: C, 53.08; H, 3.77; N, 14.66. UV-Vis λ_{max}, nm (ε, $M^{-1}\ cm^{-1}$): 249 (12 825), 304 (33 046), 357 (26 261), 366 (20 572). FT-IR (KBr, cm^{-1}): 3420 (ν_{O-H}), 3130 (ν_{C-H}), 2020 (ν_{C-H}), 1600 ($\nu_{C=C}$), 1480 ($\nu_{C=O}$), 1060 (ν_{ClO_4}), 750 (ν_{C-H}), 620 (ν_{ClO_4}).

Probing for aliphatic C–C bond cleavage reactivity involving 7-ClO$_4$. $Ni(ClO_4)_2{\cdot}6H_2O$ (7.3 mg, 0.02 mmol) was dissolved in CH_3CN (2.7 ml). This solution was added to a mixture of dibenzoylmethane (4.5 mg, 0.02 mmol) and NEt_3 (2.8 μL, 0.02 mmol). The resulting mixture was stirred for 30 min at which point it was added to MBBP (6.8 mg, 0.02 mmol). This clear green solution was stirred for 30 min. To this solution was added H_2O (300 μL) and NEt_3 (279 μL, 2.00 mmol) followed by purging with O_2 and stirring for 24 h at ambient temperature. CH_2Cl_2 (8 ml) and HCl (8 ml, 1 M) were then added, followed by stirring for 1 h and subsequently the organic layer was separated. The organic layer was dried over Na_2SO_4 and brought to dryness under vacuum to give a white solid (3.3 mg, 73% based on dibenzoylmethane). The ^1H NMR ($CDCl_3$) spectrum of the solid showed only dibenzoylmethane and no aliphatic C–C bond cleavage products.

In a separate experiment, a similar reaction was performed with the only difference being after stirring the mixture of **7-ClO$_4$** for 30 minutes in dry CH_3CN, one equivalent of NEt_3 (~3 μL, 0.02 mmol) was added. An aliquot was taken before O_2 purging and then again after stirring for 24 h at room temperature. ESI-MS of both aliquots only contained patterns for **7** and **8**. After workup using HCl and CH_2Cl_2 extraction as described above, a white solid was isolated (4.1 mg, 91%). The ^1H NMR of this solid indicated only dibenzoylmethane was isolated.

Probing for aliphatic C–C bond cleavage reactivity involving 7-Cl. The same conditions as **7-ClO$_4$** were used, except $NiCl_2{\cdot}6H_2O$ (4.8 mg, 0.02 mmol) was used instead of $Ni(ClO_4)_2{\cdot}6H_2O$ in dry CH_3CN. After adding one equivalent of NEt_3 (~3 μL, 0.02 mmol), the reaction was stirred for 10 min. An aliquot was taken before O_2 purging and then again after stirring for 24 h at room temperature. ESI-MS of both aliquots only contained patterns for **7** and **8**. After workup using HCl and CH_2Cl_2 extraction as described above, a white solid was isolated (4.0 mg, 88%). The ^1H NMR of this solid indicated only dibenzoylmethane was isolated.

Evaluation of the reactivity of 1–7 in the presence of D_2O and NEt_3 using ^1H NMR. Each isolated complex (4.09×10^{-3} mmol) was evaluated by ^1H NMR over 24 h under aerobic conditions in dry CD_3CN only (600 μL), dry CD_3CN (600 μL) containing NEt_3 (5 eq.), dry CD_3CN (540 μL) containing 10% added D_2O (60 μL), or dry CD_3CN (540 μL) containing 10% added D_2O (60 μL) and NEt_3 (5 eq.). Evaluations for complexes **5** and **6** were also done under previously published conditions (*i.e.* dried solvent, 1 eq. NEt_3).[24] Each isolated complex was evaluated by UV-vis over 24 h in $CH_3CN : H_2O$ (9 : 1) in the presence of 5 equivalents of NEt_3.

Addition of MBBP (1 eq.) to 5 in CD_3CN. Complex **5** (2.0 mg, 3.40×10^{-3} mmol) was dissolved in CD_3CN (600 μL) and a ^1H NMR spectrum was collected under paramagnetic conditions. MBBP (1.1 mg, 3.40×10^{-3} mmol) was added, the solution was briefly mixed and another ^1H NMR spectrum was collected. Additional spectra were collected after 3 h and 24 h. The NMR spectra indicated significant formation of **8**.

X-Ray crystallography. Single crystals of **1–3** and **8** were used for X-ray crystallography studies. Structures of **1**, **3** and **8** were determined at the University of Montana (UM) where a crystal of each was mounted on a glass fiber using viscous oil and transferred to a Bruker D8 Venture using Mo Kα (λ = 0.71073 Å) radiation for data collection at 100 K. The structure of **2** was determined at Utah State University. Single crystals of **2** were mounted on a glass fiber using viscous oil and transferred to a Rigaku XtaLAB Mini II Diffractometer using Mo Kα (λ = 0.71073 Å) radiation for data collection at 100 K.

1, 3 and 8. Collected data were corrected for absorption using SADABS.[32] Using Olex2,[33] the structure of each was solved with the SHELXT[34] structure solution program using direct methods and refined with the SHELXL[35] refinement package using least squares minimization. All non-hydrogen atoms were refined with anisotropic thermal parameters. For **1** the hydrogen atoms were placed in geometrically calculated positions and refined using a riding model. For **3** the hydrogen atoms attached to the heteroatoms were located in the residual electron density maps, placed, and refined with isotropic thermal parameters. All other hydrogen atoms were placed in geometrically calculated positions and refined using a riding model. For **8** all the hydrogen atoms were placed in geometrically calculated positions and refined using a riding model. Isotropic thermal parameters of riding hydrogen atoms were fixed to 1.2 times the *U* value of the atoms they are linked to (1.5 times for methyl groups). Calculations and refinement of structures were carried out using APEX2,[36] SHELXTL,[37] and Olex2[33] software.

The structure of **8** was found to contain indistinguishable solvent molecules within voids in the lattice. Attempts at modelling this solvent were not able to produce a suitable model. The SQUEEZE[38] routine within PLATON[39] was utilized to account for the residual, diffuse electron density and the model is refined against these data. A total of 27 electrons per unit cell were corrected.

2: Data were corrected for absorption using Gaussian grid (numerical integration) and a 0.5 mm 1D horizontal Gaussian beam correction for the graphite monochromator. Using Olex2,[33] the structure was solved with the SHELXT[34] structure solution program using intrinsic phasing and refined with the SHELXL[35] refinement package using least squares minimization. All non-hydrogen atoms were refined with anisotropic thermal parameters. Hydrogen atoms for **2** attached to heteroatoms were found in the residual electron density maps, placed, and refined with isotropic thermal parameters. All other hydrogen atoms for **2** were placed in geometrically calcu-

 This journal is © The Royal Society of Chemistry 2020

Published on 19 May 2020. Downloaded by Utah State University on 5/28/2020 4:39:59 PM.

lated positions and refined using a riding model. Isotropic thermal parameters of the placed hydrogen atoms were fixed to 1.2 times the U value of the atoms they are linked to (1.5 for methyl groups). Calculations and refinement of structures were carried out using CrysAlisPro,[40] SHELXL[35] and Olex2[33] software.

Compounds **1** and **3** crystallize in the monoclinic crystal system, while **2** and **8** are triclinic. The space groups for each complex were the following: **1**: $1C_{2/c}1$, **2**: $P\bar{1}$, **3**: $P12_{1/c1}$, **8**: $P1$. In **8**, three perchlorate oxygen atoms were modelled as disordered over two positions.

Results and discussion

Synthesis and characterization of TERPY-ligated Ni(II) diketonate complexes

To evaluate the solution and O_2 reactivity properties of Ni(II) diketonate complexes supported by a tridentate chelate ligand, three new TERPY-ligated complexes were prepared and characterized. Complexes **1–3** were prepared as outlined in Scheme 4 under air, with the synthesis of **1** and **2** being performed using excess diketone. Isolation of the desired diketonate complex required crystallization or precipitation of the product to separate it from $[(TERPY)_2Ni](ClO_4)_2$ (**4**), which was also formed in the reaction mixture (*vida infra*). Complexes **1–4** were characterized by X-ray crystallography, elemental analysis, ^{1}H NMR, ESI mass spectrometry, UV-vis, and FTIR (Fig. S1–S19†).

X-ray structures of 1–3

Details of the X-ray data collection and refinement for **1–3** is provided in Table S1.† Selected bond distances and angles are given in Tables S2 and S3.† Representations of the cationic portions of the X-ray structures of **1–3** are shown in Fig. 1. Each cation contains a pseudo-octahedral Ni(II) center with the meridional coordinated TERPY ligand and one diketonate

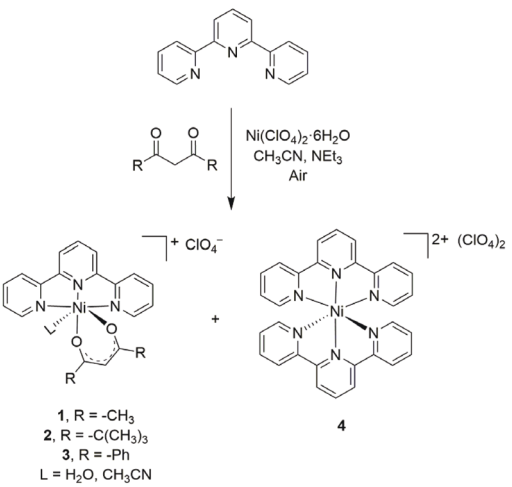

Scheme 4 The synthetic pathway for the preparation of **1–3**. Compound **4** is a contaminating species in each reaction mixture.

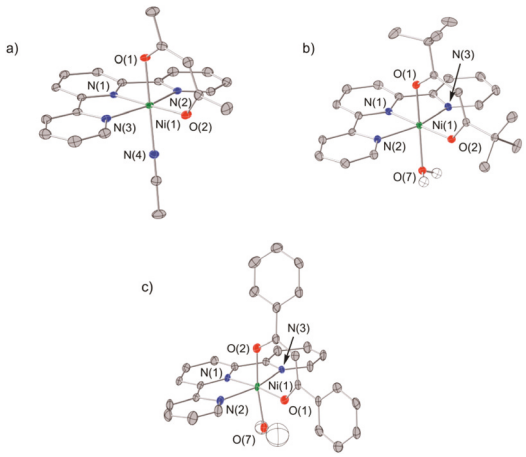

Fig. 1 Cationic portions of (a) **1**, (b) **2** and (c) **3**. Hydrogen atoms except for those of coordinated water molecules have been omitted for clarity. Ellipsoids are plotted at the 50% probability level.

oxygen donor occupying coordination positions in the equatorial plane. The other diketonate oxygen donor occupies an axial position *trans* to a coordinated solvent molecule (CH_3CN (**1**) or H_2O (**2** and **3**)). The Ni–N bond lengths for the TERPY ligand are in the range of 2.00–2.14 Å. The Ni–O(diketonate) distances are in the range of 1.98–2.05 Å. The Ni–N(CH_3CN) distance in **1** (2.09 Å) is similar to the Ni–O(H_2O) distances in **2** and **3** (2.14 and 2.09 Å, respectively). Comparison of the bond distances to those reported by Ramasubramanian *et al.* for $[(MBBP)Ni((CH_3)_3CC(O)CHC(O)C(CH_3)_3)]ClO_4$ (**5**) and [(MBBP)Ni(PhC(O)CHC(O)Ph)]Cl (**8**) revealed similar Ni–O distances and Ni–N distances.[24]

Solution characterization of 1–3

Based on prior results from our laboratory,[26] we hypothesized that the pseudo-octahedral TERPY-ligated Ni(II) diketonate complexes would be amenable to characterization by ^{1}H NMR under paramagnetic conditions. We also hypothesized that ^{1}H NMR would be a useful way to monitor the solution reactivity of these diketonate complexes. We therefore pursued studies of the ^{1}H NMR features of crystalline samples **1–3** in CD_3CN. As shown in Fig. 2, each complex exhibits signals over a range of −15 to +75 ppm. An additional broad peak is found at 132 ppm (Fig. S1–S3†). Assignment of resonances was made on the basis of integrated intensity and chemical shift considering a contact shift model.[26] The signal at 132 ppm is tentatively assigned to the pyridyl C–H atoms adjacent to the nitrogen donors. Due to the broad nature of this signal, the integrated intensity could not be determined. The signals b and c for each complex (Fig. 2) integrate to two hydrogen atoms and are assigned to the *meta* C–H positions on the terminal pyridyl donors of the TERPY ligand. A resonance at 38–39 ppm (d), which integrates to one hydrogen, is assigned to the *meta* C–H on the central pyridyl ring. Resonances at 16 (e, 1H) and 12 (f, 2H) ppm, respectively, are assigned to the *para* C–H positions of the central and terminal pyridyl rings. A signal integrating

Published on 19 May 2020. Downloaded by Utah State University on 5/28/2020 4:39:59 PM.

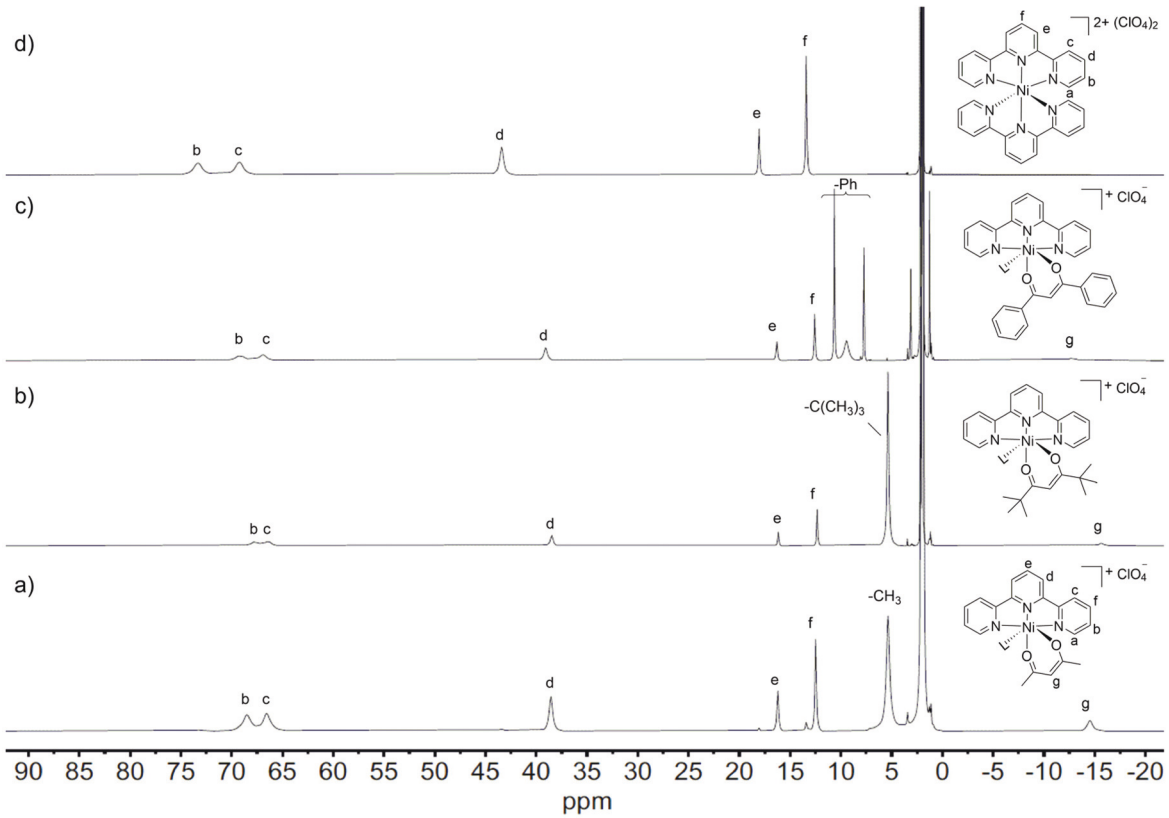

Fig. 2 ^{1}H-NMR spectra of TERPY-ligated (a) **1**, (b) **2**, (c) **3** and (d) **4** in CD_3CN.

to one hydrogen at −15 ppm is assigned as the central C–H moiety of each β-diketonate ligand. The spectrum for **1** also contains a singlet at 5.3 ppm, with an integration of six hydrogens, which is assigned to the methyl hydrogens of the acetoacetonate ligand. Complex **2** has a similar singlet with an integration of 18 hydrogens for the trimethylacetyacetonate ligand. The ^{1}H NMR spectrum of **3** contains three signals in the range of 7.7–10.7 ppm which integrate to 10 hydrogens for the phenyl hydrogens of the diketonate ligand.

Careful analysis of the ^{1}H NMR features of analytically pure **1** (Fig. 2(a)) revealed the presence of a minor impurity. The signals for this impurity match those of the bis-TERPY complex, $[(TERPY)_2Ni](ClO_4)_2$ (**4**, Fig. S4†).[30,31] Notably, evaluation of the reaction mixture filtrates (Fig. S5–S7†) remaining following isolation of the precipitated/crystalline **1–3** using ^{1}H NMR and ESI-MS indicated the presence of the diketonate complexes **1–3** as well as **4**. Analysis of crystalline samples of **1–3** in CH_3CN by ESI-MS revealed molecular ions for the $[(TERPY)Ni(diketonate)]^+$ and $[(TERPY)Ni(diketonate)(CH_3CN)]^+$ cations (Fig. S8–S10†) as well as an isotope cluster for the $[(TERPY)_2Ni(ClO_4)]^{2+}$ (**4**, Fig. S11†) cation. Overall, it is clear that **4** is formed in the reaction mixtures leading to the formation of **1–3**.

Synthesis and solution characterization of MBBP-ligated Ni diketonate complexes

Based on our experience in preparing and characterizing the $[(TERPY)Ni(diketonate)]ClO_4$ complexes (**1–3**), we examined the previously reported MPPB-ligated diketonate complexes **5–7** to evaluate: (a) is $[(MBBPNi)_2](ClO_4)_2$ (**8**) similarly present in the reaction mixtures of the $[(MBBP)Ni(diketonate)]ClO_4$ complexes? (b) Can ^{1}H NMR be used to characterize the solution properties of the MBBP-ligated diketonate complexes? Our interest in the first question stems in part from color descriptions of these previously reported compounds.[24] Specifically, the diketonate derivatives $[(MBBP)Ni(CH_3C(O)CHC(O)CH_3)]ClO_4$ (**5**), $[(MBBP)Ni((CH_3)_3CC(O)CHC(O)C(CH_3)_3)]ClO_4$ (**6**), and $[(MBBP)Ni(PhC(O)CHC(O)Ph)]Cl$ (**7-Cl**) were reported as being orange-brown solids whereas the CIF files for **6** and **7-Cl** list green crystals.[24] Our experience with the $[(TERPY)Ni(diketonate)]ClO_4$ complexes suggested that the desired diketonate complexes should be green whereas the a bis-MBBP complex $[(MBBP)_2Ni](ClO_4)_2$ (**8**) may be tan to orange-brown. In their paper, Ramasubramanian, *et al.* did briefly mentioned that the $[(MBBP)_2Ni](ClO_4)_2$ (**8**) complex is detected by ESI-MS following oxygenation of the diketonate complexes. We hypothesized that it also could be present in the reaction mixtures leading to the isolation of **5–7**.

Using the synthetic procedures under air used for the preparation of **1–3**, we attempted the synthesis of **5–7** (Scheme 5). We identified the following differences from the prior report by Ramasubramanian *et al.*, noting that their reactions were run under N_2.[24] In our hands, in each reaction mixture, a green precipitate is produced prior to Et_2O addition. As shown *via* synthetic investigations for **6**, this occurs

This journal is © The Royal Society of Chemistry 2020

Published on 19 May 2020. Downloaded by Utah State University on 5/28/2020 4:39:59 PM.

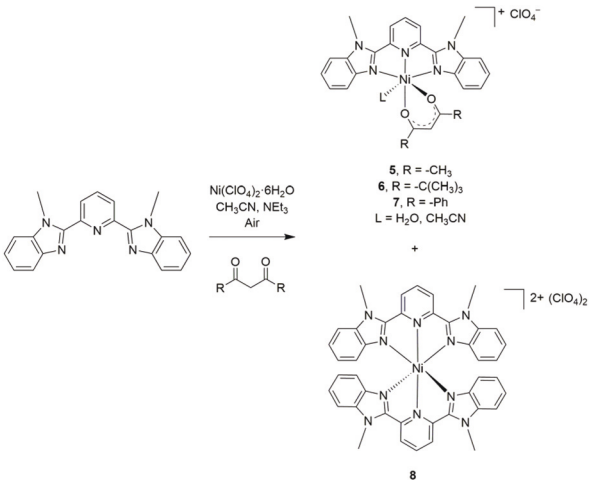

Scheme 5 Products identified in the syntheses of **5**–**7**. Complex **8** was identified in each reaction mixture using ^{1}H NMR based on an independently generated sample.

whether the reaction was run under air or N_2. Isolation and evaluation of the green solid as well as the filtrate by ^{1}H NMR (Fig. 3; Fig. S20 (R = $-CH_3$; solid) and S21 (R = $-CH_3$; filtrate); Fig. S22 (R = $-C(CH_3)_3$; solid) and S23 (R = $-C(CH_3)_3$; filtrate)) and ESI-MS (Fig. S24 and S25†) indicated that the green solids were the desired [(MBBP)Ni(diketonate)]ClO_4 complexes (**5** and **6**). ESI-MS analysis of solutions of **5** and **6** showed the presence of the $[(MBBP)_2Ni]^{2+}$ cation (Fig. S24 and S25†). The presence of this ion suggested that a trace amount may be present in the samples or that ligand exchange was occurring under the conditions of the mass spectral experiment. To fully characterize $[(MBBP)_2Ni](ClO_4)_2$ (**8**) we independently prepared the complex which was then characterized using X-ray crystallography (Fig. 4), ^{1}H NMR (Fig. S26 (CD_3CN) and S27 (d_6-DMSO)), ESI-MS (Fig. S28†), UV-vis (Fig. S29†), and FTIR (Fig. S30†). The structural features of **8** are similar to those of $[(TERPY)_2Ni](ClO_4)_2$ with Ni–N distances of 2.03–2.12 Å.[30]

The ^{1}H NMR features of **5** and **6** (Fig. 3(a) and (b)) are like those of the TERPY diketonate complexes. Resonances for the MBBP derivatives can be assigned based on integrated intensity and consideration of a primary contact shift contribution to the chemical shifts.[26] A signal at 65 ppm integrating to two hydrogens is assigned to the aryl C–H closest to each benzimidazole nitrogen donor. A sharp resonance integrating to two hydrogens at ~26 ppm is assigned to the adjacent aryl C–H moiety. Overlapping signals integrating to three hydrogens at ~15 ppm correspond to the *meta*- and *para*-hydrogens of the central pyridyl donor of the MBBP ligand. The remaining benzimidazole aryl hydrogens as well as the diketonate substituent hydrogens (except the central C–H) are found in the region of 0–10 ppm. The diketonate central C–H resonance is found at −15 ppm. We note that assignment of the ^{1}H NMR spectral features of **6** enabled us to compare the results of synthetic

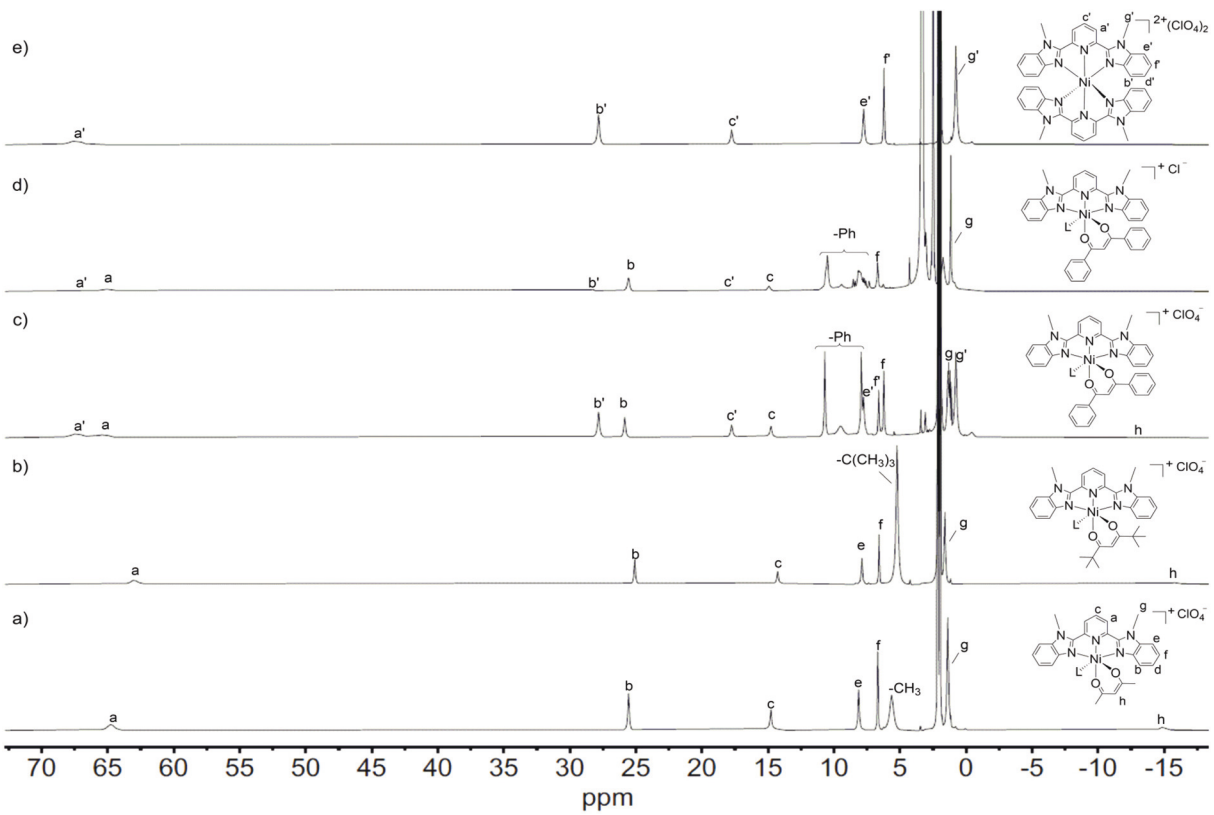

Fig. 3 ^{1}H NMR spectra of MBBP-ligated (a) **5**, (b) **6** (c) **7-ClO$_4$**, (d) **7-Cl** and (e) **8** in CD_3CN.

Published on 19 May 2020. Downloaded by Utah State University on 5/28/2020 4:39:59 PM.

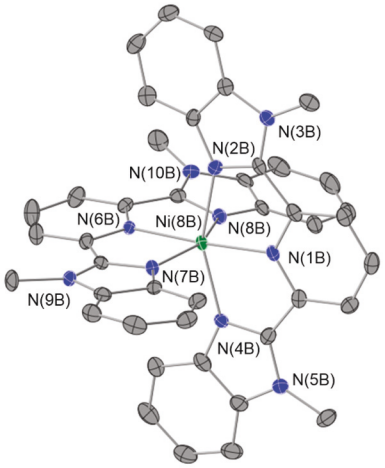

Fig. 4 Thermal ellipsoid representation of a cationic portion of the X-ray structure of **8**. The complex crystallizes with two cations per asymmetric unit. Hydrogen atoms have been omitted for clarity. Ellipsoids are plotted at the 50% probability level.

reactions performed for this complex under air and N_2. For the latter, as is shown in Fig. S31 and S32,† the ^{1}H NMR and ESI-MS features of the compound isolated under N_2 indicate that some **8** is present. The presence of the bis-MBBP complex is due to a different work up procedure being employed under N_2 that didn't enable physical separation of **6** and **8**.

Our attempts to generate the MBBP-ligated Ni(II) dibenzoylmethane derivative **7-ClO$_4$** always resulted in the isolation of mixtures of **7-ClO$_4$** with **8**. Representative ^{1}H NMR spectra of the filtrate showed neither complex (Fig. S33†), but isolated precipitate (Fig. 3(c); Fig. S34†) suggested the presence of both complexes. ESI-MS data shows the filtrate contains trace amounts of **7-ClO$_4$**, while the precipitate is consistent with a mixture of **7-ClO$_4$** and **8** (Fig. S35†). Attempted syntheses of the chloro derivative [(MBBP)Ni(PhC(O)CHC(O)Ph)]Cl (**7-Cl**) produced similar results. By ^{1}H NMR, the precipitated solid contains a mixture of **7-Cl** and **8** (Fig. 3(d); Fig. S36†). The remaining filtrate also contains trace amounts of both compounds (Fig. S37†). ESI-MS of the isolated solid and filtrate also indicates the presence of both compounds (Fig. S38†).

Exposure of complexes to H_2O/NEt_3 under aerobic conditions

Ramasubramanian *et al.* reported that exposure of **5–7** to O_2 in CH_3CN in the presence of NEt_3 (1 eq.) led to oxidative aliphatic carbon–carbon bond cleavage within the diketonate unit (52% yield). They additionally reported that the presence of 10% water produced a slightly lower yield (41%) of the aliphatic C–C bond cleavage product (benzoic acid). As we prepared and isolated analytically pure **1–6** under aerobic conditions, it was evident that the complexes were not reactive with O_2. We therefore next examined whether the addition of NEt_3 and/or water would lead to diketonate cleavage reactivity. ^{1}H NMR samples were prepared under the following conditions and were evaluated after being stored for 24 h at ambient temperature under air: (a) dry CD_3CN only; (b) dry CD_3CN + 10% D_2O; (c) dry CD_3CN + 1 eq. NEt_3 (**6** and **7** only); (d) dry CD_3CN + 5 eq. NEt_3; (e) dry CD_3CN + 10% D_2O + 5 eq. NEt_3. Spectra associated with these experiments are provided in the ESI (**1**: Fig. S39–S42; **2**: Fig. S43–S46; **3**: Fig. S47–S50; **5**: Fig. S51–S55; **6**: Fig. S56–S60†). As shown for the TERPY-ligated Ni(II) acetylacetonate complex **1** in Fig. S39–S42,† in the presence of D_2O (10%) or NEt_3 (5 eq.) a small amount of the bis-TERPY complex **4** appears to form over 24 h relative to that seen in CD_3CN alone. The amount of **4** present appears to be influenced more by the presence of NEt_3 than water. Notably, a solution containing both D_2O and NEt_3 shows the most significant amount of bis-TERPY complex (**4**) formation after 24 h (Fig. 5 and Fig. S42†). The diketonate complexes **2** and **3** exhibit similar reactivity. By ^{1}H NMR, **4** is stable with respect to the presence of D_2O (10%) and NEt_3 (5 eq.) over 24 h (Fig. S61†). Analysis of the reactivity of **1** and **4** in CH_3CN in the presence of D_2O (10%) and NEt_3 (5 eq.) at ambient temperature using UV-visible spectroscopy (Fig. S63†) shows that **4** is stable whereas **1** exhibits minor changes, possibly suggesting the formation of **4**.

The MBBP-ligated complexes **5** and **6** were exposed to the same conditions (CD_3CN, 10% D_2O, NEt_3 (5 eq.) for 24 h. As was the case for the TERPY complexes, the acetoacetonate derivative **5** showed an increase in the amount of **8** present (Fig. 6). The observed reactivity was complete with 3 h but was monitored over 24 h. The formation of **8** is also observed in solutions of **6**, although the reaction proceeds more slowly than for **5**. By ^{1}H NMR, **8** shows no change under the previously described conditions (as was observed for **4**; Fig. S62†). As was done for **1** and **4**, the reactivity was also analysed by UV-visible spectroscopy for **5** and **8** under the same conditions (CD_3CN, 10% D_2O, NEt_3 (5 eq.; Fig. S64†). While **8** displayed no change over 24 hours, **5** exhibited a small band shift after 30 minutes, with no change being observed afterward (both at 3 h and 24 h).

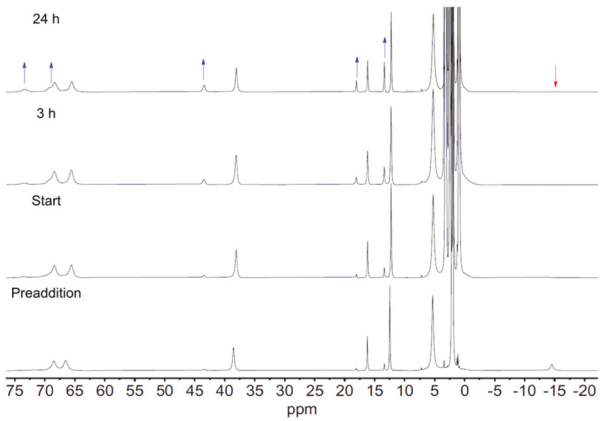

Fig. 5 ^{1}H-NMR spectra of **1** in dry CD_3CN with 10% D_2O (v : v) and excess NEt_3 (5 eq.) over time, starting with a preaddition spectrum (NEt_3 and D_2O not added) (a), a spectrum after addition of all reagents (b), 3 hours later (c) and 24 hours later (d). The blue arrow highlights the growth of **4**, and the red arrow represents the disappearance of the diketonate C–H proton.

This journal is © The Royal Society of Chemistry 2020

Published on 19 May 2020. Downloaded by Utah State University on 5/28/2020 4:39:59 PM.

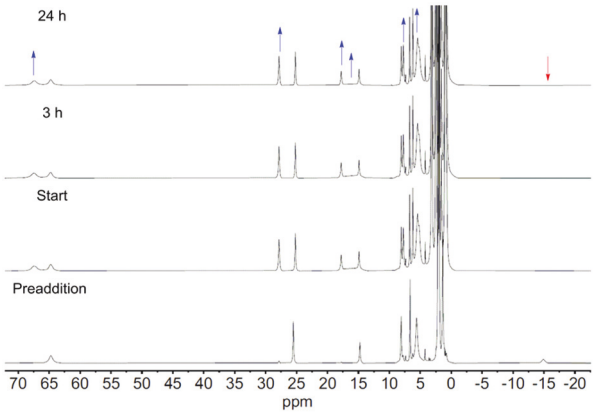

Fig. 6 ^{1}H-NMR stacked spectra of **5** in CD_3CN with 10% D_2O and excess NEt_3 over time, starting with a pre-addition spectrum (NEt_3 and D_2O not added) (a), a spectrum after addition of all reagents (b), 3 hours later (c) and 24 hours later (d). The blue arrow highlights the growth of **8**, and the red arrow represents the disappearance of the α proton.

Notably, addition of TERPY (1 eq.) to a CD_3CN solution of **1** showed significant conversion to **4** (Fig. S65†). This indicates that free TERPY appears to be able to displace the diketonate ligand. In a similar experiment involving addition of MBBP (1 eq.) to a CD_3CN solution of **5**, growth of signals for **8** can also be observed (Fig. S66†).

Evaluation of aliphatic C–C bond cleavage reactivity

To probe for aliphatic C–C bond cleavage, we stirred an CH_3CN solution of **3** containing 10% H_2O (v : v) and NEt_3 (100 eq.) for 24 h at ambient temperature after purging with O_2. Exposure of the solution to 1 M HCl followed by extraction with CH_2Cl_2 resulted in the isolation of unaltered dibenzoylmethane (71% recovery, Fig. S67†). A similar experiment performed using an *in situ*-generated sample of [(MBBP)Ni(PhC(O)CHC(O)Ph)]ClO_4 (**7-ClO$_4$**) also resulted only in the isolation of unaltered dibenzoylmethane (73% recovery, Fig. S68†). Notably, an experiment performed using **3**, **7-ClO$_4$**, or **7-Cl** in the presence of 1 eq. NEt_3 as reported by Ramasubramanian *et al.*[24] produced only unreacted dibenzoylmethane (71%–91%, Fig. S69–S74†) after 24 h stirring and acidic workup.

Stability of Ni(II) diketonate complexes under CH_3CN/aqueous basic conditions

Both sets of tridentate Ni(II) diketonate complexes are stable when exposed to O_2 both as solids and in CH_3CN solution. This is evident as: (1) these complexes can be synthesized and isolated *in air*; and (2) no oxidative products were identified or isolated from solutions under aerobic conditions. These results are consistent with literature precedent, which suggests that only Ni(II) complexes containing an electron rich diketonate ligand exhibit oxidative C–C bond cleavage reactivity with O_2.[15–23] Some evidence was found for potential ligand exchange reactivity wherein the tridentate Ni(II) diketonate complexes were converted to bis MBBP or bis TERPY Ni(II) complexes in solution. The exchange reactivity is enhanced for diketonate complexes with less steric hinderance.

Conclusions

Oxidative aliphatic C–C bond cleavage reactions of diketones mediated by first-row divalent metals and involving O_2 are of current interest.[9–23] The highest level of oxidative cleavage reactivity has been found for electron rich Ni(II) diketonates. The recent reactivity reported for a MBBP-ligated Ni(II) aryl diketonate complex drew our interest due to the oxidative cleavage of a non-substituted diketone upon reaction with O_2.[24] Typically Ni(II) complexes of an unsubstituted aryl diketonate are air stable.[20] We have been unable to reproduce these results with either MBBP- or TERPY-supported Ni(II) diketonate complexes. Instead, these complexes are stable in air, and in aerobic CH_3CN/aqueous basic conditions or CD_3CN/NEt_3 only exhibit some possible ligand exchange reactivity.

Conflicts of interest

The authors declare no conflict of interest.

Acknowledgements

We thank the National Science Foundation (CHE-1664977 to LMB; CHE-1429195 for Brüker Avance III HD 500 MHz NMR; CHE-1828764 for Rigaku Benchtop XtaLAB Mini II X-ray diffractometer). X-ray crystallographic studies of **1**, **3** and **8** were performed at the University of Montana X-ray diffraction core facility, which is supported by the Center for Biomolecular Structure and Dynamics CoBRE (National Institutes of Health, CoBRE NIGMS P20GM103546). Single crystal X-ray diffraction data were collected using a Bruker D8 Venture (NSF MRI CHE-1337908).

References

1 N. Vodnala, R. Gujjarappa, C. K. Hazra, D. Kaldhi, A. K. Kabi, U. Beifuss and C. C. Malakar, *Adv. Synth. Catal.*, 2019, **361**, 135–145.
2 P. R. Sakhare, P. Subramanian and K. P. Kaliappan, *J. Org. Chem.*, 2019, **84**, 2112–2125.
3 M. Wang, J. Ma, H. Liu, N. Luo, Z. Zhao and F. Wang, *ACS Catal.*, 2018, **8**, 2129–2165.
4 H. Liu, M. Feng and X. Jiang, *Chem. – Asian J.*, 2014, **9**, 3360–3389.
5 Y. Liang and N. Jiao, *Acc. Chem. Res.*, 2017, **50**, 1640–1653.
6 F. Chen, T. Wang and N. Jiao, *Chem. Rev.*, 2014, **114**, 8613–8661.
7 C. J. Allpress and L. M. Berreau, *Coord. Chem. Rev.*, 2013, **257**, 3005–3029.

Published on 19 May 2020. Downloaded by Utah State University on 5/28/2020 4:39:59 PM.

8 G. D. Straganz, A. Glieder, L. Brecker, D. W. Ribbons and W. Steiner, *Biochem. J.*, 2003, **369**, 573–581.
9 A. R. Diebold, G. D. Straganz and E. I. Solomon, *J. Am. Chem. Soc.*, 2011, **133**, 15979–15991.
10 A. R. Diebold, M. L. Neidig, G. R. Moran, G. D. Straganz and E. I. Solomon, *Biochemistry*, 2010, **49**, 6945–6952.
11 G. D. Straganz and B. Nidetzky, *J. Am. Chem. Soc.*, 2005, **127**, 12306–12314.
12 I. Siewert and C. Limberg, *Angew. Chem., Int. Ed.*, 2008, **47**, 7953–7956.
13 H. Park, M. M. Bittner, J. S. Baus, S. V. Lindeman and A. T. Fiedler, *Inorg. Chem.*, 2012, **51**, 10279–10289.
14 S. Banerjee and T. K. Paine, *Inorg. Chim. Acta*, 2020, **501**, 119200.
15 S. Hoof, M. Sallmann, C. Herwig, B. Braun-Cula and C. Limberg, *Dalton Trans.*, 2017, **46**, 16792–16795.
16 E. Szajna, A. M. Arif and L. M. Berreau, *J. Am. Chem. Soc.*, 2005, **127**, 17186–17187.
17 L. M. Berreau, T. Borowski, K. Grubel, C. J. Allpress, J. P. Wikstrom, M. E. Germain, E. V. Rybak-Akimova and D. L. Tierney, *Inorg. Chem.*, 2011, **50**, 1047–1057.
18 C. J. Allpress, K. Grubel, E. Szajna-Fuller, A. M. Arif and L. M. Berreau, *J. Am. Chem. Soc.*, 2013, **135**, 659–668.
19 S. Raje, K. Mani, P. Kandasamy, R. J. Butcher and R. Angamuthu, *Eur. J. Inorg. Chem.*, 2019, 2164–2167.
20 E. Szajna-Fuller, K. Rudzka, A. M. Arif and L. M. Berreau, *Inorg. Chem.*, 2007, **46**, 5499–5507.
21 C. J. Allpress, A. M. Arif, D. T. Houghton and L. M. Berreau, *Chem. – Eur. J.*, 2011, **17**, 14962–14973.
22 C. J. Allpress, A. Milaczewska, T. Borowski, J. R. Bennett, D. L. Tierney, A. M. Arif and L. M. Berreau, *J. Am. Chem. Soc.*, 2014, **136**, 7821–7824.
23 S. L. Saraf, A. Milaczewska, T. Borowski, C. D. James, D. L. Tierney, M. Popova, A. A. Arif and L. M. Berreau, *Inorg. Chem.*, 2016, **55**, 6916–6928.
24 R. Ramasubramanian, K. Anandababu, M. Kumar and R. Mayilmurugan, *Dalton Trans.*, 2018, **47**, 4049–4053.
25 M. da Graça M. B. Martin, M. Hörner, M. B. Behm and F. S. Nunes, *Z. Anorg. Allg. Chem.*, 2011, **637**, 1229–1233.
26 E. Szajna, P. Dobrowolski, A. L. Fuller, A. M. Arif and L. M. Berreau, *Inorg. Chem.*, 2004, **43**, 3988–3997.
27 D. B. G. Williams and M. Lawton, *J. Org. Chem.*, 2010, **75**, 8531–8354.
28 I. Mathew and W. Sun, *Dalton Trans.*, 2010, **39**, 5885–5898.
29 W. C. Wolsey, *J. Chem. Educ.*, 1973, **50**, 335–337.
30 A. T. Baker, D. C. Craig and A. D. Rae, *Aust. J. Chem.*, 1995, **48**, 1373–1378.
31 C. Anderer, C. Näther and W. Bensch, *IUCrData*, 2016, **1**, x161009.
32 G. M. Sheldrick, *SADABS: Area Detector Absorption Correction*, University of Göttingen, Germany, 1996.
33 O. V. Dolomanov, L. J. Bourhis, R. J. Gildea, J. A. K. Howard and H. Puschmann, *J. Appl. Crystallogr.*, 2009, **42**, 339–341.
34 G. M. Sheldrick, *Acta Crystallogr., Sect. A: Found. Adv.*, 2015, **71**, 3–8.
35 G. M. Sheldrick, *Acta Crystallogr., Sect. C: Struct. Chem.*, 2015, **71**, 3–8.
36 Bruker, *APEX3*, Bruker AXS Inc., Madison, Wisconsin, USA, 2016.
37 G. M. Sheldrick, *Acta Crystallogr., Sect. A: Found. Crystallogr.*, 2008, **64**, 112–122.
38 A. L. Spek, *Acta Crystallogr.*, 2015, **C71**, 9–18.
39 A. L. Spek, *Acta Crystallogr.*, 2009, **D65**, 148–155.
40 *CrysAlisPRO*, Oxford Diffraction/Agilent Technologies UK Ltd, Yarnton, England.

This journal is © The Royal Society of Chemistry 2020